Journal of Tissue Engineering
Volume 10: 1–9

DOI: 10.1177/2041731419831466
journals.sagepub.com/home/tej
SAGE

In vivo bone regeneration by differently designed titanium membrane with or without surface treatment: a study in rat calvarial defects

Yong-Seok Jang[1], So-Hee Moon[2], Thuy-Duong Thi Nguyen[3], Min-Ho Lee[1], Tae-Ju Oh[4], A-Lum Han[5] and Tae-Sung Bae[1]

Abstract

The current objective was to evaluate six groups of titanium membranes in a rat calvarial defect model, regarding the surface treatment with or without calcium-phosphate coating and surface topography with no, small, or large holes. Critical size defects (Φ = 8 mm, n = 42) were surgically created in rat calvaria, and then were treated by one of the six groups. Biopsies were obtained at 4 weeks (n = 5 per group) for micro-computed tomography and histomorphometric analyses. Fluorochrome bone markers were injected in two rats each group at 1 (Alizarin red), 3 (Calcein green) and 5 weeks (Oxytetracyclin yellow), followed by histological examination at 7 weeks to assess bone regeneration dynamic. At 4 weeks, the highest bone volume was observed in no-hole groups independent of surface treatment ($p < 0.05$). Treated groups with no-hole and large-hole membranes showed increased bone mineral density than with respective non-treated groups ($p < 0.05$). Histology exhibited an intimate bone formation onto the treated membranes, whereas non-treated ones demonstrated interposition of connective tissue, which was confirmed through bone contact percentages. The results suggest that occlusive membranes showed more bone formation than other perforated ones, and calcium-phosphate treatment induces intimate bone formation toward the membrane.

Keywords

Calcium-phosphate coating, titanium membrane, bone regeneration, surface treatment, rat calvarial model

Date received: 27 September 2018; accepted: 25 January 2019

Introduction

Bone regeneration using titanium mesh with various pore sizes ranging from micrometers to millimeters and natural or synthetic polymer membranes together has been employed to promote bone augmentation prior to implant placement by maintaining a space while preventing soft-tissue proliferation.[1–3] Titanium (Ti) membranes have the following advantages when being used for bone regeneration: promote bone regeneration, maintain space efficiently, cause less infection, and fit over the shape of defect.[3–5] It has been reported that holes/pores present in barrier membranes promote osteogenesis by maintaining the blood supply in the transplanted area and surgical stability by aiding tissue integration and extracellular nutrition variances.[6,7] However, the perforation penetration of

[1]Department of Dental Biomaterials, Institute of Oral Bioscience and Institute of Biodegradable Material, BK21 Plus Project, School of Dentistry, Chonbuk National University, Jeonju, South Korea
[2]Department of Periodontology, School of Dentistry, Chonbuk National University, Jeonju, South Korea
[3]Faculty of Odonto-Stomatology, Hue University of Medicine and Pharmacy, Hue, Vietnam
[4]Department of Periodontics and Oral Medicine, School of Dentistry, University of Michigan, Ann Arbor, MI, USA
[5]Department of Family Medicine, College of Medicine, Wonkwang University, Iksan, South Korea

Corresponding author:
Tae-Sung Bae, Department of Dental Biomaterials, Institute of Oral Bioscience and Institute of Biodegradable Material, BK21 Plus Project, School of Dentistry, Chonbuk National University, 664-14 Deokjin-dong, Jeonju 561-756, South Korea.
Email: bts@jbnu.ac.kr

connective tissue may occur through the holes, hindering bone regeneration.[8,9] Therefore, identifying an optimal pore size that will prevent excessive soft-tissue ingrowth and enhance bone regeneration is critical.

Recently, surface treatment on Ti is often considered to induce earlier growth of osseous tissue before soft-tissue proliferation.[10–16] In our previous study, effects of surface modification of an occlusive Ti membrane on promoting its osseointegration have been investigated.[17] The surface treatment is based on changing the nanoscale topography of Ti surface and loading the bioactive calcium-phosphate (Ca-P) particles onto the surface via anodization, precalcification, and heat treatment (APH treatment). In comparison with non-treated Ti membranes, the precalcificated ones exhibit higher bioactivity and an increase in bone formation with high bone density toward the membrane.[17] Meanwhile, pristine Ti with a spontaneous Ti oxide film layer on the surface takes a long time for the osteoblast to attach and form contact bone regeneration.[4,6,10,12,18,19] Thus, soft-tissue interposition found between the Ti membrane and the new bone slows down the bone growth and remodeling.[17]

Referring to the result that the APH treatment of Ti foil could promote new bone formation with high bone density in vivo in comparison with bare Ti foil in our previous study,[17] the present study proposes a hypothesis that surface treatment can induce an early direct bone formation on perforated Ti membranes, inhibiting soft-tissue penetration through the holes. Besides that, two kinds of hole size were investigated to optimize the perforation of Ti mesh. Therefore, this study was conducted to investigate the influence of various designs of Ti membranes on bone regeneration with regard to surface treatment through a rat calvarial defect model.

Experimental materials and methods

Preparation of specimens

Circular Ti plates (thickness: 80 μm, Φ: 10 mm; Neoplant, Neobiotech Co, Ltd, Korea) were prepared and divided into six study groups (n = 7 per group) depending on surface treatment of no treatment (NT) or APH treatment (APH), and morphologies for three kinds of Ti mesh: no hole (NH), small hole (SH), or large hole (LH): APH-NH, APH-SH, APH-LH, NT-NH, NT-SH, and NT-LH (Figure 1). Holes were created throughout the membrane surface by selective laser melting with two different diameters, 0.4 ± 0.01 mm for SH and 1.5 ± 0.01 mm for LH. The ratio of the holed area to the entire area was equally maintained at 20%. The APH treatment was carried on through three sequential treatment steps: anodization, cyclic precalcification and heating, which was described before.[13] Briefly, a nanotube array was first formed on Ti substrate by anodization treatment in Glycerol solution at 20 V for 1 h.

(a)

Surface treatment	Surface design	Groups
Non treatment	No hole	NT-NH
	Small hole	NT-SH
	Large hole	NT-LH
APH treatment	No hole	APH-NH
	Small hole	APH-SH
	Large hole	APH-LH

(b)

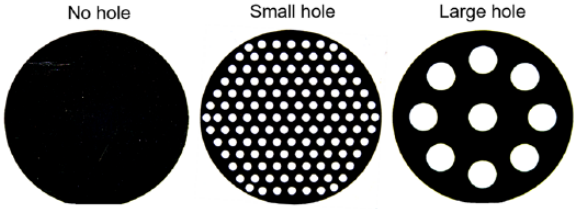

Figure 1. (a) Six study groups depending on surface treatment and surface topography and (b) morphologies for three kinds of Ti mesh: no hole (NH), small hole (SH), and large hole (LH).

Subsequently, cyclic precalcification was performed for 20 cycles to load Ca and P particles on this nanotubular layer. Finally, to stabilize formed structure, the specimens were heat-treated at 500°C for 2 h. The morphological microstructure of treated surface was observed using a field emission–scanning electron microscope (FE-SEM, S800, Hitachi, Japan), and the chemical elements on the surface after APH treatment were analyzed using energy dispersive X-ray spectroscopy (EDS, Bruker, USA).

Animal preparation and surgical procedures

A total of 42 8-week-old Sprague-Dawley rats (#300 g) were used. This in vivo study was conducted in compliance with the principles of the Helsinki Declaration. Ethical clearance of the study was approved by the Institutional Animal Care and Use Committee. Under general anesthesia, the periosteum was incised and lifted to expose the calvarium after incision of the skin. A critical-size defect of 8 mm in diameter in each rat cranium was formed using a trephine bur connected to an endodontic motor (X-SMARTTM, Densply, Japan) under profuse irrigation. These calvarial defects were treated by seven membranes per group, respectively, to completely cover the bone defect. The periosteum was replaced and sutured with bioabsorbable silk (5-0 Polyglactin 910 (Vicryl), Ethicon, Livingston, UK). Finally, the skin was sutured with a 4/0 suture silk (4/0 Black silk, Ailee Co, Busan, Korea). Antibiotics was administered subcutaneously (300 μL/kg) at 0, 24, and 48 h. After 4 weeks, five rats per group were sacrificed by an overdose of thiopental (ChoongWae Pharma, Seoul, Korea). Tissue blocks (20 × 20 mm) containing the specimen were extracted, stored in saline, and analyzed immediately by micro-computed tomography (micro-CT).

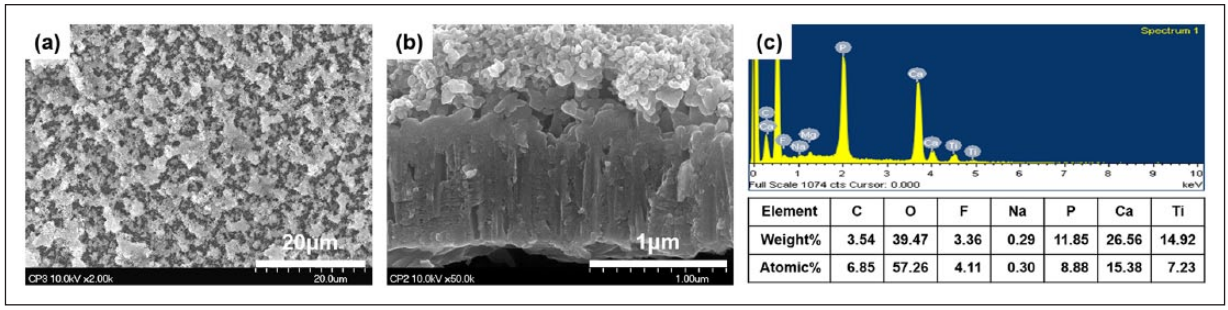

Element	C	O	F	Na	P	Ca	Ti
Weight%	3.54	39.47	3.36	0.29	11.85	26.56	14.92
Atomic%	6.85	57.26	4.11	0.30	8.88	15.38	7.23

Figure 2. FE-SEM images of treated Ti membranes (small-hole surface): (a) surface view (magnification ×2000) showed a homogeneous and porous coating with Ca-P granules. (b) cross-sectional view (magnification ×50,000) revealed that this coating contains two parts: a below nanotubular array which was penetrated by above Ca-P precipitations, and (c) chemical elements on the surface after APH treatment analyzed by EDS.

Micro-CT evaluation

The tissue blocks were scanned using micro-CT (Skyscan 1076, Skyscan, Kontich, Belgium) at 100 kV, 100 μA. X-ray images were obtained using the NRecon software (Skyscan). Regions of interest (ROIs) were bounded to create a range and included all tissue beneath the Ti membrane along the cranial defect boundary, which was 8 mm in diameter. The osseous tissue had a threshold of 80–200 in Hounsfield unit. Three-dimensional images were built using the CTVol program (Skyscan). Bone volume (BV) and bone mineral density (BMD) were measured using the CTAn software (Skyscan).

Histomorphometric analysis

Calvaria blocks were fixed in 10% formalin, stained in Villanueva solution (Polysciences, Inc., Warrington, PA, USA), dehydrated and embedded with methyl methacrylate. The resin blocks were cut perpendicularly to the plane of Ti membrane through the center point. Then, the obtained slides were ground to 40 μm and observed using an optical microscope (DM2500, Leica Microsystem, Wetzlar, Germany). The percentage of bone–membrane contact (BMC%) over the total length of the sectioned membrane was measured by an image analysis program (ImageJ, America National Institutes of Health, Bethesda, MD, USA).

Bone formation dynamic analysis

To clearly understand the bone regeneration process under the Ti membrane, continuous fluorescent labeling was carried out for two rats from each group. Red Alizarin complexone of 25 mg/kg (Sigma, St. Louis, MO, USA), green Calcein of 25 mg/kg (Sigma, St. Louis, MO, USA), and yellow Oxytetracycline of 20 mg/kg (Sigma, St. Louis, MO, USA) were administered at 1, 3, and 5 weeks after surgery by subcutaneous injection, respectively. Then, 7 weeks later, tissue blocks were obtained, and resin-embedded sections were produced as the above method. Fluorescent-stained ossification was observed using a confocal laser-scanning microscope (CLSM 510 Meta, Zeiss, Jena, Germany).

Statistical analysis

BV, BMD, and BMC% were presented as the mean ± standard deviation. For the statistical analysis, Tukey's post hoc test and one-way analysis of variance (ANOVA) were carried out using SPSS software (version 12.0, SPSS, Chicago, IL, USA). Statistical significance was recognized if the p value <0.05.

Results

After APH treatment, the Ti membrane surface was covered by a homogeneous and porous coating with Ca-P granules (Figure 2). Same surface characteristics were found in no-hole, small-hole, and large-hole surfaces. Ca of 15.38% and P of 8.88% were detected on the surface after APH treatment of Ti membrane, and Ca/P atomic ratio was 1.73, which is the similar rate to 1.67 of hydroxyapatite (HAp).

Micro-CT evaluation

As show in Micro-CT images after in vivo test during 4 weeks (Figure 3), the defects in no-hole groups was completely covered with new bone. New bones in groups with small and large holes were grown toward the center of the defect from old bone edges, and the generation amount of bone was smaller than that of the no-hole group. In comparison with non-treated groups, bones covered a bit more area on the surfaces of the treated groups.

BV and BMD calculated by micro-CT evaluation after in vivo test were summarized in Table 1. There was no significant difference between the treated group and non-treated group in terms of BV (Figure 4(a)). However, the BV values of no-hole membranes were higher than those

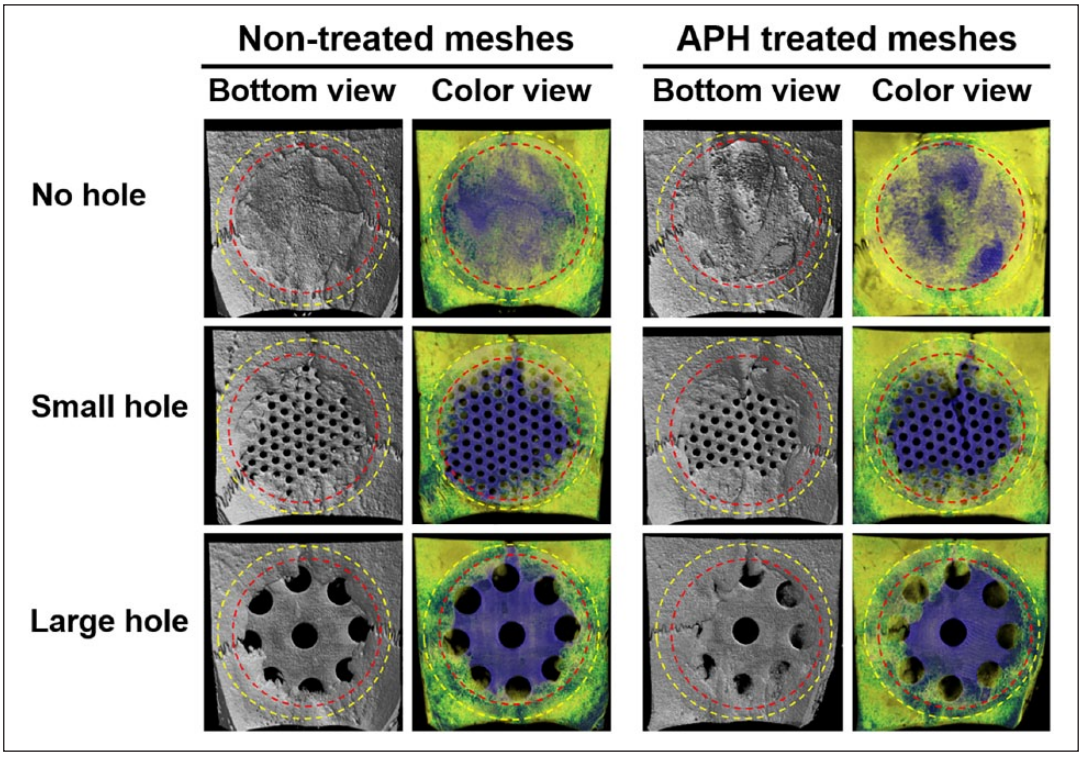

Figure 3. Micro-CT images after in vivo test.
Yellow-dotted line indicates Ti membrane and red dotted line indicates the critical-size defects formed in rat craniums.

Table 1. Bone volume and bone mineral density calculated by micro-CT evaluation on bone regeneration within the regions of interest.

Group	BV		BMD	
	Mean	SD	Mean	SD
NT-NH	11.52	1.97	747.07	28.01
NT-SH	6.33	0.75	791.55	27.08
NT-LH	6.93	1.07	760.96	29.75
APH-NH	10.99	0.78	854.37	18.88
APH-SH	7.50	1.57	803.38	19.68
APH-LH	7.40	1.80	827.05	26.61

BV: bone volume; BMD: bone mineral density; SD: standard deviation; NT: no treatment; NH: no hole; SH: small hole; LH: large hole; APH: anodization, precalcification, and heat.

of other perforated membranes ($p < 0.05$). Meanwhile, considering the BMD values (Figure 4(b)), treated group showed a higher value than non-treated group in no-hole and large-hole Ti membranes ($p < 0.05$).

Histomorphometry

As shown in Figure 5, new bone layer formed in the defect along the connective tissue but not in contact with membrane in all NT groups. In addition, even though the defect was completely covered with new bone in NT-NH group, new bone had low density like trabecular bone including bone marrow cells. Meanwhile, in APH groups, bone formed directly along membrane, growing from old bone edges to the center of the defect. Especially, the defect was closed completely in APH-NH group even though new bone did not completely bridge the defects in the APH-SH and APH-LH groups. New bones with high density, like cortical bones, formed directly along membrane in the APH groups.

The BMC% values (Figure 6) for non-treated membranes are 0%, which means that new bone have little contact with membranes due to the connective tissue. Meanwhile, the APH-treated groups showed high BMC% values, and APH-NH and APH-SH groups showed higher BMC% than APH-LH group did ($p < 0.05$).

Osteogenesis dynamic

At 7 weeks, the three fluorescent labels (Alizarin red, Calcein green, and Oxytetracycline yellow) were observed, marking the bone formation dynamic at 1, 3, and 5 weeks, respectively (Figure 7). These three labels in merged images were mixed together in some areas which indicate that deformation/remodeling of new bone layers occurred continuously during the healing time. Under the treated membranes, the fluorescent labels appeared directly in contact with the membrane, regardless of whether holes were present or not. Meanwhile, the thicker extending

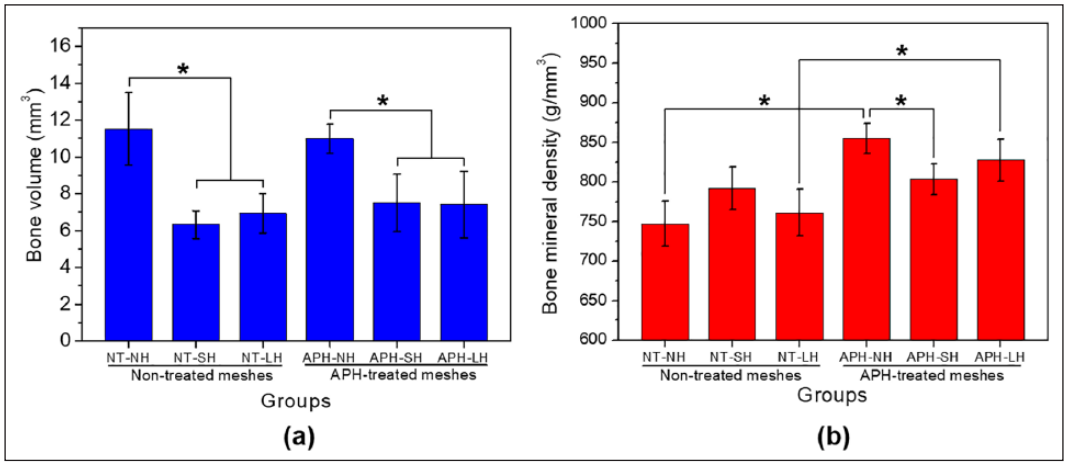

Figure 4. Quantitative results of the micro-CT evaluation on bone regeneration within the regions of interest: (a) bone volume and (b) bone mineral density.
*Significant difference between groups ($p < 0.05$).

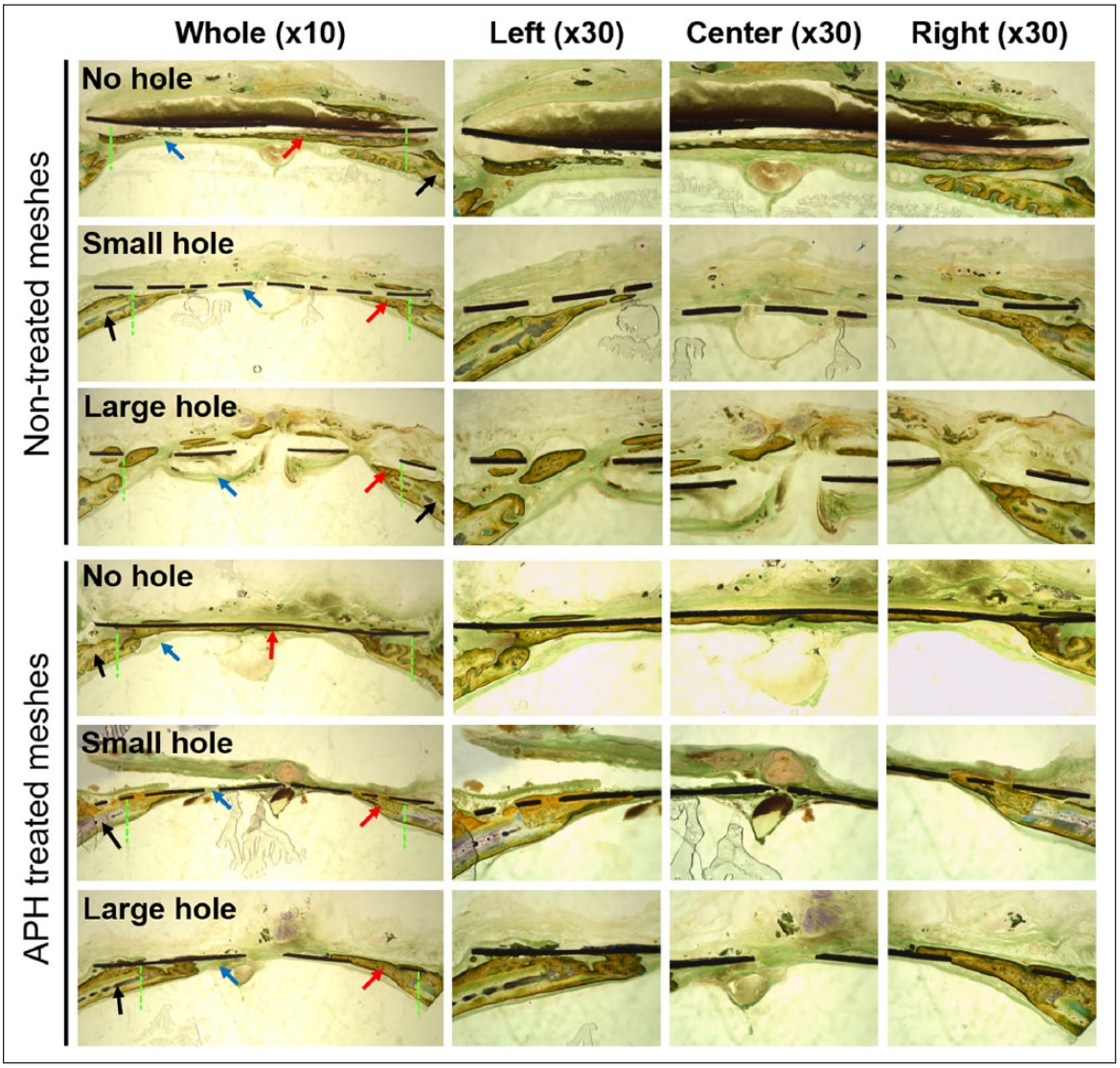

Figure 5. Cross-sectional images (magnification ×10 and ×30) through the center points of non-treated membranes and APH-treated membranes after Villanueva bone staining.
Original defect area is between green dotted lines. Black, red, and blue arrows indicate the old bone, new bone, and connective tissue, respectively.

labels were separately observed from the non-treated membranes. In the APH-treated groups, the 1-week label (red) was observed to be in direct contact with the membrane surface, followed by the 3-week label (green) and 5-week label (yellow). This phenomenon indicates that the sequence of bone formation began directly on the treated Ti membrane and proceeded outward. Whereas, the labels of mineralized tissue formed under NT-SH and NT-LH groups were observed in an opposite order: the 5-week label was closer to membranes than the 3-and 1-week labels. In the NT-NH group, the new bone formed spontaneously away from the membrane. Thus, it is speculated that the APH-treated membranes promoted intimate bone regeneration directly from the membrane and oriented the ossification. The dynamics of bone regeneration are not affected by the hole size of the membrane.

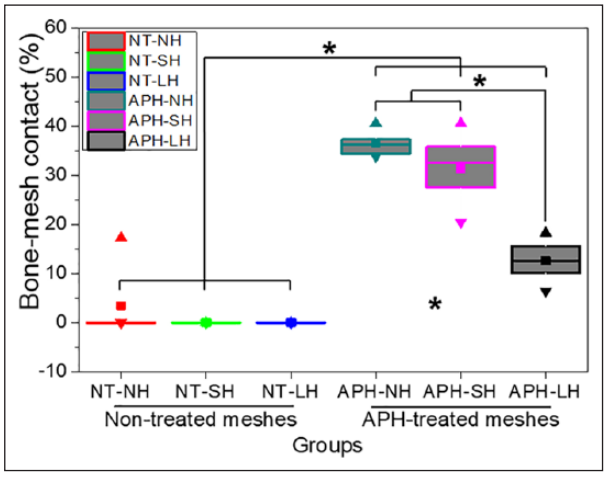

Figure 6. Bone–membrane contact (BMC) percentage (%). *significant difference between groups ($p < 0.05$). ■: mean value; ▲: maximum value; ▼: minimum value, boxes and line in boxes showed interquartile range (50%) and median.

Discussion

In this study, three designs of Ti membranes (NH, SH, and LH) with or without APH surface treatment were tested on a rat calvarial defect model, and then quantitative and qualitative evaluations for bone regeneration were conducted. The investigated results revealed that the volume of bone formation was negatively affected by the presence of perforations on the membranes, while the volume and

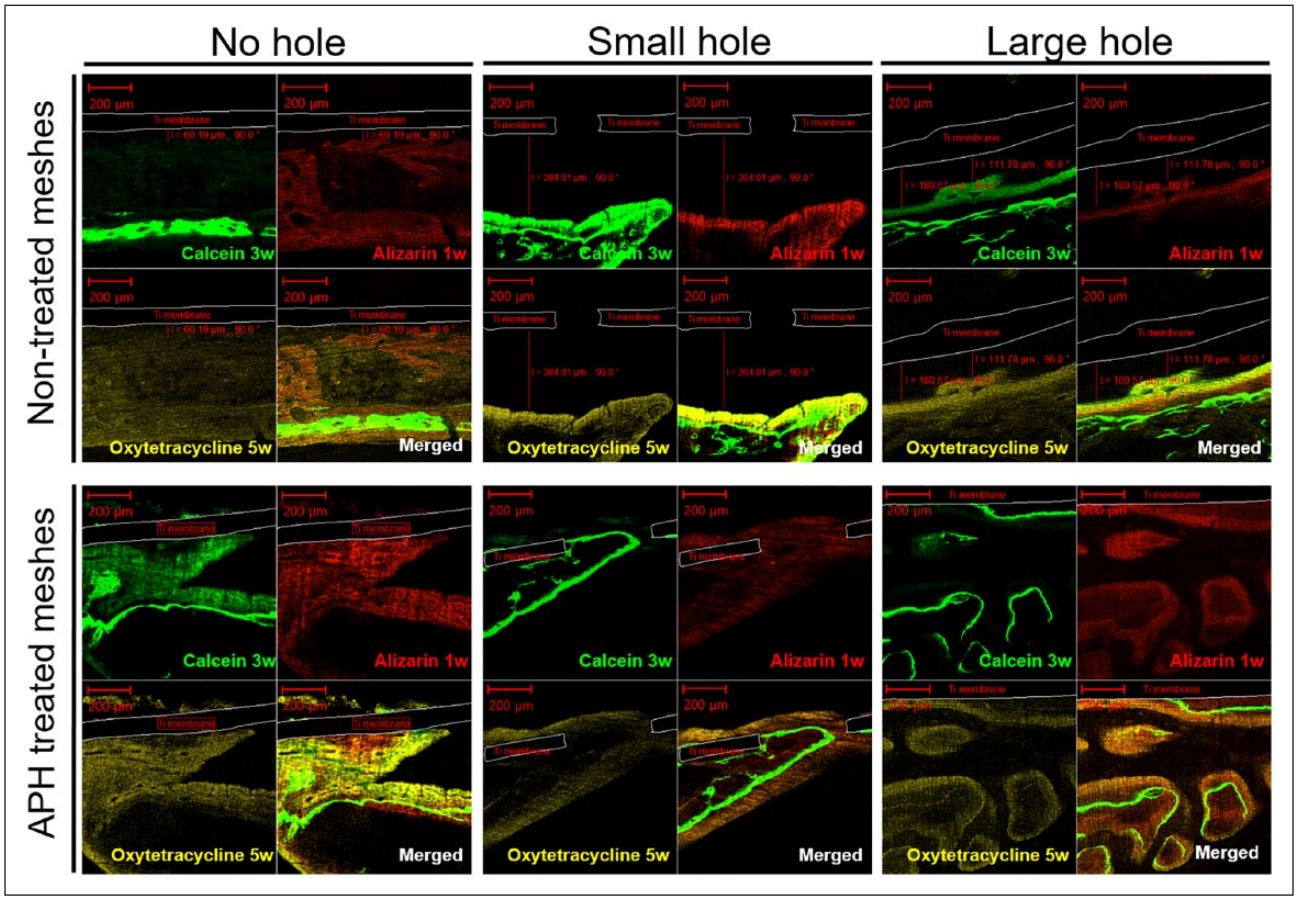

Figure 7. Postoperative fluorescence microphotograph (magnification ×100) at 7 weeks: Alizarin labels at 1 week (red, right-above), Calcein labels at 3 weeks (green, left-above), Oxytetracycline labels at 5 weeks (yellow, left-below) and merged images. The fluorescent images were taken around the center areas where new bone layer were found under Ti membranes.

density of newly formed bone were increased by APH treatment.

In the results of our recent study,[17] the APH-treated surfaces showed direct bone deposition under the membrane surfaces and growing along with the membrane. Meanwhile, connective tissue formed at 2 weeks under non-treated surfaces, followed by apposition of bone growth at 4 weeks, and incorporation of the connective tissue and bone was observed at 10 weeks, which was quantified through BMC% calculation. In this study, regardless of the membrane designs, treated membranes showed higher BMC% than non-treated membranes. In addition, the observed osteogenic dynamic from 1 to 7 weeks postoperatively is consistent with previous evaluation.[17] It appeared that the bone regeneration originated from the treated membrane surfaces, followed by new bone growth toward the defect area over time. On the contrary, the osteogenesis occurred from the defect to the non-treated barrier membrane over time due to the hindrance of the interposed soft-tissue layer between the new bone and this membrane. It can be speculated that Ca- and P-enriched Ti surface promoted the bone formation and prevented the interposition of soft tissues.[14,20] In consideration of bone-quality assessment by micro-CT, our previous study found that lower BV but higher BMD in the treated occlusive membrane than non-treated one at 8 weeks.[17] In addition, this phenomenon was reconfirmed through recent study conducted using the surface modification of Ti-Ta-Mo-Zr alloy.[21] In this study, the similar BV and higher BMD values were detected in APH-NH and APH-LH groups than NT-NH and NT-LH groups even though BMD values between NT-LH and APH-SH groups showed no statistically significant difference. Thus, it can be argued that the ossification process of bone regeneration were enhanced by the surface treatment.

With regard to physio-biological function of a barrier in ossseoregeneration, occlusive and perforated membranes were evaluated in this study. Compared to perforated Ti membranes, the newly formed BV was significantly higher in occlusive Ti membranes. Meanwhile, the difference in BMD values between non-treated and treated groups was statistically significant, but BMD values between no-hole and hole groups showed statistically insignificant difference, except small-hole groups. In addition, BMC% values of treated groups were significantly higher than non-treated groups. Thus, it was identified that the occlusive membranes allowed more bone formation than perforated ones, and APH treatment affected BMD and BMC in healing time. In this study, new bone formation on APH groups was accelerated, since the synthetization of osteoid material by differentiated osteoblast cells and the mineralization of osteoid were promoted by supplying abundant calcium from the surface of treated Ti membrane.[22,23] Thus, the surface of APH groups was rapidly covered with new bone which had higher BMD.

Lundgren et al.[24] reported that the occlusive Ti plate prevented infiltration of the soft tissue, leading to successful ossseoregeneration. In a rabbit experiment, Schmid et al.[25] concluded that membrane permeability was unnecessary for guided bone regeneration. However, it has been suggested that occlusive membranes may block the penetration of nutrients and growth-regulatory factors into the protected site, increasing the frequency of soft-tissue dehiscence and thereby resulting in exposure of the barrier membrane.[3,6] Further studies are needed to clarify the exact mechanism of cell occlusive function of Ti membrane.

Several studies have been performed to investigate the effect of pore size on the absorbable barrier membrane during fibrous tissue penetration and osteogenesis.[26–30] Chvapil et al.[26] claimed that quick penetration of vascular connective tissue can be expected only when the pore size is a minimum of 100 μm, and Taylor and Smith[27] proposed that pores with an average size of 42 μm cannot penetrate capillary vessels. Other studies reported that pores larger than 100 μm are required for the growth of osseous tissue, while pores larger than 150 μm are required for the formation of osteon.[29,30] For Ti mesh membrane, Rakhmatia and colleagues[31,32] reported that higher new bone was formed in micro-porous Ti mesh with 50 μm in pore diameter than in commercially available macro-porous Ti mesh with 1700 μm in pore diameter in early stage bone healing in a canine model, but more bone formation with lower BMD had occurred in Ti mesh with larger pores (Φ=1700 μm) than small pores (Φ=20, 50, 100 μm) even though soft-tissue ingrowth had occurred in Ti mesh with 100 μm in pore diameter in the rat calvarial defect model. In addition, Hasegawa et al.[33] developed micro-porous Ti mesh with 20 μm in pore diameter and found that particulate autogenous bone in all defects at alveolar bones of the mandibles was replaced with mature osseous tissue through remodeling without adhesion to the surrounding tissue. Since these results were obtained using Ti meshes without surface treatment, larger pore size was used in this study to find out how rapidly the bone covers the pore in Ti mesh through fast bone healing in early stage by APH treatment, which can result in formation of new bone layer in contact with membrane without any soft tissue between the bone and the mesh.

In this study, two types of perforated Ti membranes were used as follows: a small-hole group (Φ=0.4 mm), which is mainly used in clinical trials, and a large-hole group with an increased hole size (Φ=1.5 mm). Insignificant differences in BV and BMD were found between the small- and large-hole groups. This result is similar to the result of other studies, in which the difference in the amount of bone growth between small- and large-pore-sized meshes was insignificant and unlikely to result in any practical or meaningful clinical consequence.[34,35] In this study, the perforated area percentage was equally maintained at 20% for both two designs, leading to no difference of the BV and BMD values between the two groups. However, if considering each hole

on Ti mesh is an unsupported site, the small-hole group has the same unsupported area but higher supported points in comparison with large-hole group. In the unsupported site, the bone has to grow from the margin to the center of the hole to heal the defect under it. Larger hole needs more time to close the hole than small hole.[34,35] This hypothesis might have explained why BMC% value of SH group was superior to LH group ($p < 0.05$). This finding is consistent with the study of Gutta et al.,[35] where mineral apposition rate was found to be the lowest in the large-pore-mesh group. Thus, even with the same porosity area, there might have been better bone healing beneath the mesh with small hole size than with large hole size.

Conclusion

In summary, regardless of the surface treatment, the occlusive Ti membrane showed more bone formation than other perforated ones at 4 weeks. New bone with high density formed directly along membrane in APH-treated groups, better bone healing was identified in APH-treated Ti mesh with small hole than in APH-treated Ti mesh with large hole. The Ca-P coating through APH treatment may induce early contact bone formation and change the bone regeneration dynamic on the Ti membrane, which was independent of the barrier design.

Acknowledgements

Both Y.-S. J. and S.-H.M. contributed equally to this work and are considered as joint first author.

Declaration of conflicting interests

The author(s) declared no potential conflicts of interest with respect to the research, authorship, and/or publication of this article.

Funding

The author(s) disclosed receipt of the following financial support for the research, authorship, and/or publication of this article: This work was supported by the National Research Foundation of Korea (NRF) grant funded by the Korea government (MSIP) (grant no.: 2012R1A2A2A01012671).

ORCID iD

Tae-Sung Bae https://orcid.org/0000-0002-8307-4544

References

1. Mayfield L, Nobreus N, Attstrom R, et al. Guided bone regeneration in dental implant treatment using a bioabsorbable membrane. *Clin Oral Implants Res* 1997; 8(1): 10–17.
2. Rasia-dalPolo M, Poli PP, Rancitelli D, et al. Alveolar ridge reconstruction with titanium meshes: a systematic review of the literature. *Med Oral Patol Oral Cir Bucal* 2014; 19(6): e639–e646.
3. Rakhmatia YD, Ayukawa Y, Furuhashi A, et al. Current barrier membranes: titanium mesh and other membranes for guided bone regeneration in dental applications. *J Prosthodont Res* 2013; 57(1): 3–14.
4. Her S, Kang T and Fien MJ. Titanium mesh as an alternative to a membrane for ridge augmentation. *J Oral Maxillofac Surg* 2012; 70(4): 803–810.
5. Damiati L, Eales MG, Nobbs AH, et al. Impact of surface topography and coating on osteogenesis and bacterial attachment on titanium implants. *J Tissue Eng*. Epub ahead of print 2 August 2018. DOI: 10.1177/2041731418790694.
6. Weng D, Hurzeler MB, Quinones CR, et al. Contribution of the periosteum to bone formation in guided bone regeneration. *Clin Oral Implants Res* 2000; 11(6): 546–554.
7. Linde A, Thoren C, Dahlin C, et al. Creation of new bone by an osteopromotive membrane technique: an experimental study in rats. *J Oral Maxillofac Surg* 1993; 51(8): 892–897.
8. Simion M, Trisi P, Maglione M, et al. A preliminary report on a method for studying the permeability of expanded polytetrafluoroethylene membrane to bacteria in vitro: a scanning electron microscopic and histological study. *J Periodontol* 1994; 65(8): 755–761.
9. Lundgren AK, Lundgren D and Taylor A. Influence of barrier occlusiveness on guided bone augmentation. *Clin Oral Implants Res* 1998; 9(4): 251–260.
10. Albrektsson T, Sennerby L and Wennerberg A. State of the art of oral implants. *Periodontol* 2000 2008; 47: 15–26.
11. Davies JE. Mechanisms of endosseous integration. *Int J Prosthodont* 1998; 11(5): 391–401.
12. Cooper LF, Masuda T, Yliheikkila PK, et al. Generalizations regarding the process and phenomenon of osseointegration. *Int J Oral Maxillofac Implants* 1998; 13(2): 163–174.
13. Nguyen Moon SH, Oh TJ, Park IS, et al. The effect of APH treatment on surface bonding and osseointegration of Ti-6Al-7Nb implants: an in vitro and in vivo study. *J Biomed Mater Res B Appl Biomater* 2015; 103(3): 641–648.
14. Franco Rde L, Chiesa R, de Oliveira PT, et al. Bone response to a Ca- and P-enriched titanium surface obtained by anodization. *Braz Dent J* 2008; 19(1): 15–20.
15. Wang X, Zakaria O, Madi M, et al. Vertical osteoconductivity of sputtered hydroxyapatite-coated mini titanium implants after dura mater elevation: rabbit calvarial model. *J Tissue Eng*. Epub ahead of print 30 June 2015. DOI: 10.1177/2041731415592075.
16. Orapiriyakul W, Young PS, Damiati L, et al. Antibacterial surface modification of titanium implants in orthopaedics. *J Tissue Eng*. Epub ahead of print 25 July 2018. DOI: 10.1177/2041731418789838.
17. Nguyen TD, Moon SH, Oh TJ, et al. Comparison of guided bone regeneration between surface-modified and pristine titanium membranes in a rat calvarial model. *Int J Oral Maxillofac Implants* 2016; 31: 581–590.
18. Davies JE. Understanding peri-implant endosseous healing. *J Dent Educ* 2003; 67(8): 932–949.
19. Islam MT, Felfel RM, Abou Neel EA, et al. Bioactive calcium phosphate–based glasses and ceramics and their biomedical applications: a review. *J Tissue Eng*. Epub ahead of print 21 July 2017. DOI: 10.1177/2041731417719170.
20. Fernandez de Grado G, Keller L, Idoux-Gillet Y, et al. Bone substitutes: a review of their characteristics, clinical use, and perspectives for large bone defects manage-

ment. *J Tissue Eng*. Epub ahead of print 4 June 2018. DOI: 10.1177/2041731418776819.
21. Nguyen PMH, Won D-H, Kim B-S, et al. The effect of two-step surface modification for Ti-Ta-Mo-Zr alloys on bone regeneration: an evaluation using calvarial defect on rat model. *Appl Surf Sci* 2018; 442: 630–639.
22. Fernandez-Tresguerres-Hernandez-Gil I, Alobera-Gracia MA, del-Canto-Pingarron M, et al. Physiological bases of bone regeneration II. The remodeling process. *Med Oral Patol Oral Cir Bucal* 2006; 11(2): E151–E157.
23. Matsuoka H, Akiyama H, Okada Y, et al. In vitro analysis of the stimulation of bone formation by highly bioactive apatite- and wollastonite-containing glass-ceramic: released calcium ions promote osteogenic differentiation in osteoblastic ROS17/2.8 cells. *J Biomed Mater Res* 1999; 47(2): 176–188.
24. Lundgren D, Lundgren AK, Sennerby L, et al. Augmentation of intramembraneous bone beyond the skeletal envelope using an occlusive titanium barrier. *Clin Oral Implants Res* 1995; 6(2): 67–72.
25. Schmid J, Hammerle CH, Olah AJ, et al. Membrane permeability is unnecessary for guided generation of new bone. *Clin Oral Implants Res* 1994; 5(3): 125–130.
26. Chvapil M, Holusa R, Kliment K, et al. Some chemical and biological characteristics of a new collagen–polymer compound material. *J Biomed Mater Res* 1969; 3(2): 315–332.
27. Taylor DF and Smith FB. Porous methyl methacrylate as an implant material. *J Biomed Mater Res* 1972; 6(1): 467–479.
28. Klawitter JJ, Bagwell JG, Weinstein AM, et al. An evaluation of bone growth into porous high density polyethylene. *J Biomed Mater Res* 1976; 10(2): 311–323.
29. Spector M, Flemming WR and Kreutner A. Bone growth into porous high-density polyethylene. *J Biomed Mater Res* 1976; 10(4): 595–603.
30. Welsh RP, Pilliar RM and Macnab I. Surgical implants. The role of surface porosity in fixation to bone and acrylic. *J Bone Joint Surg Am* 1971; 53: 963–977.
31. Rakhmatia YD, Ayukawa Y, Furuhashi A, et al. Microcomputed tomographic and histomorphometric analyses of novel titanium mesh membranes for guided bone regeneration: a study in rat calvarial defects. *Int J Oral Maxillofac Implants* 2014; 29(4): 826–835.
32. Rakhmatia YD, Ayukawa Y, Jinno Y, et al. Micro-computed tomography analysis of early stage bone healing using micro-porous titanium mesh for guided bone regeneration: preliminary experiment in a canine model. *Odontology* 2017; 105(4): 408–417.
33. Hasegawa H, Masui S and Ishihata H. New microperforated pure titanium membrane created by laser processing for guided regeneration of bone. *Br J Oral Maxillofac Surg* 2018; 56(7): 642–643.
34. Bobyn JD, Stackpool GJ, Hacking SA, et al. Characteristics of bone ingrowth and interface mechanics of a new porous tantalum biomaterial. *J Bone Joint Surg Br* 1999; 81(5): 907–914.
35. Gutta R, Baker RA, Bartolucci AA, et al. Barrier membranes used for ridge augmentation: is there an optimal pore size. *J Oral Maxillofac Surg* 2009; 67(6): 1218–1225.